

An Adaptive Task-Related Component Analysis Method for SSVEP recognition

Vangelis P. Oikonomou^a

^a*Information Technologies Institute, Centre for Research and Technology
Hellas, Thessaloniki, Thessaloniki, 57001, Greece*

Abstract

Steady-state visual evoked potential (SSVEP) recognition methods are equipped with learning from the subject's calibration data, and they can achieve extra high performance in the SSVEP-based brain-computer interfaces (BCIs), however their performance deteriorate drastically if the calibration trials are insufficient. This study develops a new method to learn from limited calibration data and it proposes and evaluates a novel adaptive data-driven spatial filtering approach for enhancing SSVEPs detection. The spatial filter learned from each stimulus utilizes temporal information from the corresponding EEG trials. To introduce the temporal information into the overall procedure, an multitask learning approach, based on the bayesian framework, is adopted. The performance of the proposed method was evaluated into two publicly available benchmark datasets, and the results demonstrated that our method outperform competing methods by a significant margin.

Keywords: Steady State Visual Evoked Potentials, EEG, Task related Component Analysis, Multi-task learning, Spatial Filtering, Brain Computer Interfaces

1. Introduction

A Brain Computer Interface (BCI) system is a device that it translates human brain activity into artificially generated control signals, providing us with an alternative communication medium, other than physical communication, which can be used to help people with motor disabilities [1], to augment communication abilities of healthy individuals,[2], for entertainment [2], and, for neuromarketing purposes[3]. Brain activity can be measured with various specialized devices such as MRI scanners and electroencephalograms

(EEG)-based devices, where, EEG devices is widely used since the required equipment is simple and inexpensive. EEG-based BCI systems utilize various brain responses such as motor imagery and visual responses, from which, the use of Steady State Visual Evoked Potentials (SSVEPs) have attracted the attention of many researchers due to their lower training requirements for the end-user and higher information transfer rates [4, 5]. When an individual is looking into a visual stimulus, which is flashing as a fixed frequency, then a brain response is revealed in occipital and occipital - parietal areas of individual's brain which is called SSVEP response[6]. A SSVEP response contains sinusoidal components which are related to the fundamental frequency of the visual stimulus as well as its harmonics. The overarching goal of a SSVEP BCI system is to detect the different frequency components corresponding to the visual stimuli and translate them into commands, by using an EEG-based pattern recognition algorithms.

The recognition of SSVEP responses involves the use of Machine Learning (ML) algorithms. Linear classifiers such as Support Vector Machines (SVMs) and the Linear Discriminant Analysis (LDA) have been used to detect SSVEPs [7]. In addition, in [8] the use of Multivariate Linear Regression (MLR) was proposed to learn discriminative features for improving SSVEP classification, while, in [9] kernel - based extensions of MLR were proposed using SSVEP-related kernels as an integral part of the Sparse Bayesian Learning (SBL) framework. Furthermore, Deep Learning (DL) approaches using Convolutional Neural Networks (CNN), based on time frequency analysis, are used to discriminate SSVEP responses [10, 11].

However, SSVEP responses present specific frequency and spatial characteristics, hence methods utilizing these characteristics have been proposed. More specifically, methods based on Power Spectrum Density Analysis (PSDA) were widely used for frequency detection [12], where the target frequency is assigned to the frequency corresponding to maximum value of PSD. However, the efficient calculation of PSD requires a relatively large time window, and it is sensitive to noise [13, 14]. To avoid the above shortcomings of PSDA, spatial filtering approaches have been proposed. In [14] the Minimum Energy Combination (MEC) method has been proposed while in [13] the Canonical Correlation Analysis (CCA) method was introduced. Both methods use sinusoids waves as reference templates and they solve an optimization problem, based on multi-channel SSVEP data, in order to obtain optimal spatial filters. Finally, extensions of CCA have been proposed in [15, 16, 17, 18, 19, 20], extracting the subject-specific and task-related information from the individ-

ual calibration data and reduce the effect of spontaneous background EEG activities.

From spatial filtering methods, the task-related component analysis (TRCA)-based method [18] shows great potential since it has achieved superior performance among various spatial filtering methods. The core idea of TRCA is to acquire the spatial filters by strengthening the task-related SSVEP components and suppressing the noise. TRCA-based methods are followed by the target detection step where the similarity between the filtered test signal and the filtered template is calculated via the correlation coefficient. All spatial filtering - based methods are based on the basic (generalized) eigenvalue problem [21, 22]. However, difference between various approaches can be observed and these difference are reflected to the way that the matrices, involved in the eigenvalue problem, are constructed [22]. In [23] Correlated Component Analysis (CORCA) assumes that the task related component is shared among the subjects by adopting a transfer learning procedure in the construction of covariance matrices. While, in [24] a task discriminant component analysis was applied which involves the construction of within and between SSVEP targets covariance matrices.

One defect of TRCA is that it can only deal with limited noise components. For other kinds of noise, such as locally occurring noises that have the same profile, the TRCA-based method is powerless[25, 26]. Additionally, its performance deteriorate drastically if the calibration trials are insufficient. To deal with more general noises and the number of trials, we introduce a novel adaptive time-domain filter resulting in more reliable similarity measurement. By introducing the temporally-based filter into the objective function of the TRCA-based method we construct a time filter that acts together with the spatial filter to suppress more general noises. Furthermore, the filter adapts to the statistical properties of SSVEP trials.

The rest of this paper is organized as follows. In section 2, first, we provide a short description of CCA and TRCA concentrating on the mathematical formulation of them, and then, we describe our approach for SSVEP recognition. Section 3, we describe the SSVEP datasets that are used in our study, and then we provide details about our experiments and the performance of our method. Also, a comparison with competing methods is provided. Finally, a short discussion and some concluding remarks are provided in section 4.

2. Materials and Methods

2.1. Problem Description

When a SSVEP experiment is taken place, the subject is seated in front of a screen where visual stimuli are flashing in different frequencies, During the experiment raw EEG data are collected in order to calibrate the overall system. The segmentation of raw EEG data (using event triggers), results into a set of trials for each visual stimulus (or class). Using these EEG trials the experimenter can calibrated the BCI system (for example, by training the classifier). Let us assume that the SSVEP dataset is a collection of multi-channel EEG trials $\{\mathbf{X}_1^{(s)}, \mathbf{X}_2^{(s)}, \dots, \mathbf{X}_M^{(s)}\}_{s=1}^{N_s}$ for each participant, where M is the number of trials of a SSVEP target, (s) is the index of the SSVEP target, N_s is the number of SSVEP targets (or classes). Each $\mathbf{X}_m^{(s)}, m = 1, \dots, M, s = 1, \dots, N_s$ is a matrix of $N_{ch} \times N_t$, where N_{ch} is the number of channels and N_t the number of samples. Additionally, we assume that the multi-channel EEG signals are centralized since in practise the EEG trials are bandpass filtered or detrended.

2.2. Canonical Correlation Analysis (CCA)

Spatial filtering attempts to maximize the SNR between the raw EEG data and the spatial filtered version of them. In typical cases, such as bipolar combination or laplacian filtering, the spatial filters are determined manually. However, this approach does not take into account any prior knowledge about SSVEPs or any subject-specific information. One of the first approach that take into consideration the structure of SSVEPs was based on Canonical Correlation Analysis (CCA)[13]. The CCA is a multivariate statistical method attempting to discover underlying correlations between two sets of data[13, 27]. These two sets of data is assumed to be only a different view (or representation) of the same original (hidden) data. More specifically, CCA finds a linear projection for each set such that these two set are maximally correlated in the hidden (dimensionality-reduced) space.

In the SSVEP problem these two views is the test EEG trial $\mathbf{X}_m^{(s)}$ and the

reference templates for s -th stimulus $\mathbf{Y}_{(f_s)}$, where

$$\mathbf{Y}_{(f_s)} = \begin{bmatrix} \sin(2\pi \cdot 1 \cdot f_s t) \\ \cos(2\pi \cdot 1 \cdot f_s t) \\ \vdots \\ \sin(2\pi \cdot N_h \cdot f_s t) \\ \cos(2\pi \cdot N_h \cdot f_s t) \end{bmatrix}^\top$$

$\mathbf{Y}_{(f_s)} \in \mathbb{R}^{N_t \times 2N_h}$, f_s is the frequency of s -th stimulus

Typically, CCA methods maximize the linear correlation between the projections $\mathbf{w}_s^\top \mathbf{X}_m^{(s)}$ and $\mathbf{v}_s^\top \mathbf{Y}_{f_s}$, where $\mathbf{w}_s \in \mathbb{R}^{N_{ch}}$ and $\mathbf{v}_s \in \mathbb{R}^{N_t}$. At the end, we solve the following optimization problem:

$$\max \rho_s = \max_{\mathbf{w}_s, \mathbf{v}_s} \frac{\mathbf{w}_s^\top \mathbf{X}_m^{(s)} \mathbf{Y}_{f_s}^\top \mathbf{v}_s}{\sqrt{\mathbf{w}_s^\top \mathbf{X}_m^{(s)} (\mathbf{X}_m^{(s)})^\top \mathbf{w}_s \mathbf{v}_s^\top \mathbf{Y}_{f_s} \mathbf{Y}_{f_s}^\top \mathbf{v}_s}} \quad (1)$$

Since ρ_s is invariant to the scaling of \mathbf{w}_s and \mathbf{v}_s the above optimization problem can be also formulated as the following generalized eigenvalue problem:

$$\mathbf{X}_m^{(s)} \mathbf{Y}_{f_s}^\top (\mathbf{Y}_{f_s} \mathbf{Y}_{f_s}^\top)^{-1} \mathbf{Y}_{f_s} (\mathbf{X}_m^{(s)})^\top \mathbf{w}_s = \lambda_s \mathbf{X}_m^{(s)} (\mathbf{X}_m^{(s)})^\top \mathbf{w}_s \quad (2)$$

where λ_s is the eigenvalue corresponding to the eigenvector \mathbf{w}_s .

In order to find the stimulus of test EEG trial $\mathbf{X}_m^{(s)}$, that the subject intends to select, we find ρ_s for all available stimuli and the stimulus-target, c , is then identified by finding the index of the maximum feature among N_s features: $c = \arg \max_s \{\rho_s\}$. It must be observed here that there is no need for training (or calibration) since the templates \mathbf{Y}_{f_s} are artificially generated.

2.3. Task Related Component Analysis (TRCA)

Task-related component analysis (TRCA) enhances reproducibility of SSVEPs across multiple trials and the intuition of TRCA is to maximize the reproducibility of SSVEP target-related components after spatial filtering. More specifically, the TRCA method find the spatial filters \mathbf{w}_s by solving a generalized eigenvalue problem which is described by the following equation:

$$\max_{\mathbf{w}_s} \frac{\mathbf{w}_s^\top \mathbf{A} \mathbf{A}^\top \mathbf{w}_s}{\mathbf{w}_s^\top \mathbf{B} \mathbf{B}^\top \mathbf{w}_s} \quad (3)$$

where $A = \frac{1}{M} \sum_{m=1}^M \mathbf{X}_m^{(s)}$, and B is a concatenated matrix contains all trials of s -th stimulus, $B = [\mathbf{X}_1^{(s)}, \mathbf{X}_2^{(s)}, \dots, \mathbf{X}_M^{(s)}]$.

In order to find the target of the test trial, \mathbf{X}_{test} we apply the following discriminant function:

$$c = \arg \max_s \{corr(\mathbf{w}_s^\top \mathbf{X}_{test}, \mathbf{w}_s^\top A)\} \quad (4)$$

where $corr(\cdot, \cdot)$ denotes the Pearson's correlation coefficient.

2.4. Adaptive Task-Related Component Analysis (adTRCA)

In our work we propose a new generalized eigenvalue problem for SSVEP detection which is described by the following equation:

$$\max_{\mathbf{w}_s} \frac{\mathbf{w}_s^\top A C A^\top \mathbf{w}_s}{\mathbf{w}_s^\top B D B^\top \mathbf{w}_s} \quad (5)$$

where C and D are "filtering" matrix that acts on the time dimension of trials. The matrices C and D can be defined using various approaches and their goal is to remove noise in time domain.

In our study we make some critical assumptions about the generation model of SSVEP responses, which affect the data analysis procedure. More specifically, SSVEP responses contains strong sinusoids components [13], hence the SSVEP signal in each channel is modeled as a linear combination of sinusoids described the following matrix:

$$\Phi = [\mathbf{Y}_{(f_1)} \mathbf{Y}_{(f_2)} \dots \mathbf{Y}_{(f_{N_s})}] \in \mathbb{R}^{N_t \times (2N_s N_h)}.$$

Additionally, SSVEP responses belonging to the same visual stimulus share common components. From the above we can observe that the generation of SSVEP responses can be modeled as multiple regression tasks that share common information.

EEG trials from the s -th stimulus are collected in matrix $\mathbb{B} = [\mathbf{X}_1^{(s)\top}, \mathbf{X}_2^{(s)\top}, \dots, \mathbf{X}_M^{(s)\top}]^\top$, $\mathbb{B} \in \mathbb{R}^{N_t \times (N_{ch} N_s)}$, where each column of \mathbb{B} contains the data from one channel or each column of \mathbb{B} contains the data from one task. Hence we have $\mathbf{y}_i \in \mathbb{R}^{N_t \times 1}$, $i = 1, \dots, N_{ch} N_s$ tasks (the i -th column of \mathbb{B}). Each learning task can be described by the following linear regression model:

$$\mathbf{y}_i = \Phi \mathbf{w}_i + \mathbf{e}_i \quad (6)$$

where \mathbf{w}_i $2N_sN_h \times 1$ vector of weights (or parameters), and, \mathbf{e}_i $N_t \times 1$ vector of noise coming from a zero mean Gaussian random variable with unknown precision (inverse variance) a_0 . We can observe that each of the mapping yields a corresponding regression task, and performing multiple such learning tasks has been referred to as multitask learning [28], which aims at sharing information effectively among multiple related tasks. In a more abstract view of our problem we can see that each learning task is a linear regression problem, and sinusoids components from one regression task affect the fitting procedure of another regression task.

The likelihood function for parameters \mathbf{w}_i and a_0 is given by:

$$p(\mathbf{y}_i|\mathbf{w}_i, a_0) = (2\pi a_0)^{-\frac{N_t}{2}} \exp \left\{ -\frac{a_0}{2} \|\mathbf{y}_i - \Phi \mathbf{w}_i\|_2^2 \right\} \quad (7)$$

The parameters of a regression task, \mathbf{w}_i , are assumed to be drawn from a product of zero-mean Gaussian distributions that are shared by all tasks. Letting $w_{i,j}$ be the j -th parameters for i -th task then we have:

$$p(\mathbf{w}_i|\mathbf{a}) = \prod_{j=1}^{2N_sN_h} \mathcal{N}(w_{i,j}|0, a_i^{-1}) \quad (8)$$

where the hyperparameters $\mathbf{a} = \{a_j\}_{j=1,2,\dots,2N_sN_h}$ are shared among $N_{ch}N_s$ regression tasks, hence, data from all regression tasks contribute to learning these hyperparameters. To promote sparsity over parameters, we place Gamma priors over hyperparameters \mathbf{a} [29, 28]. Also, the same type of prior is placed over noise precision a_0 .

$$\begin{aligned} p(a_0|\alpha, \beta) &= Ga(a_0|\alpha, \beta) \\ &= \frac{\beta^\alpha}{\Gamma(\alpha)} a_0^{\alpha-1} \exp \left\{ -\beta a_0 \right\} \end{aligned} \quad (9)$$

$$p(\mathbf{a}|c, d) = \prod_{j=1}^{2N_sN_h} Ga(a_j|c, d) \quad (10)$$

In addition, we can observed here, that noise properties are shared among different tasks (i.e. the noise vectors in Eq. (6) are drawn from the same Gaussian distribution). Finally, it must be noted that we have an hierarchical model, and these types of models are natural to be "dealt" within the bayesian framework.

Given hyperparameters \mathbf{a} and noise precision a_0 , we can apply Bayes theorem to find the posterior distribution over \mathbf{w}_i , which is a Gaussian distribution:

$$\begin{aligned} p(\mathbf{w}_i|\mathbf{y}_i, \mathbf{a}, a_0) &= \frac{p(\mathbf{y}_i|\mathbf{w}_i, a_0)p(\mathbf{w}_i|\mathbf{a})}{\int p(\mathbf{y}_i|\mathbf{w}_i, a_0)p(\mathbf{w}_i|\mathbf{a})d\mathbf{w}_i} \\ &= \mathcal{N}(\mathbf{w}_i|\boldsymbol{\mu}_i, \boldsymbol{\Sigma}_i) \end{aligned} \quad (11)$$

where

$$\boldsymbol{\mu}_i = a_0 \boldsymbol{\Sigma}_i \boldsymbol{\Phi}^T \mathbf{y}_i \quad (12)$$

$$\boldsymbol{\Sigma}_i = \left(a_0 \boldsymbol{\Phi}^T \boldsymbol{\Phi} + \mathbf{A} \right)^{-1} \quad (13)$$

and $\mathbf{A} = \text{diag}(a_1, a_2, \dots, a_M)$.

In order to find hyperparameters \mathbf{a} and promote sparsity in parameters, the type-II Maximum Likelihood procedure is adopted [29, 30], where the objective is to maximize the marginal likelihood (or its logarithm). Also, a similar procedure is followed for the noise precision. The marginal likelihood $\mathcal{L}(\mathbf{a}, a_0)$ is given by:

$$\begin{aligned} \mathcal{L}(\mathbf{a}, a_0) &= \sum_{i=1}^L \log \int p(\mathbf{y}_i|\mathbf{w}_i, a_0)p(\mathbf{w}_i|\mathbf{a})d\mathbf{w}_i \\ &= -\frac{1}{2} \sum_{i=1}^L \left(N_i \log(2\pi) + \log |\mathbf{C}_i| + \mathbf{y}_i^T \mathbf{C}_i^{-1} \mathbf{y}_i \right) \end{aligned} \quad (14)$$

where $\mathbf{C}_i = a_0^{-1} \mathbf{I} + \boldsymbol{\Phi} \mathbf{A} \boldsymbol{\Phi}^T$

Differentiating $\mathcal{L}(\mathbf{a}, a_0)$ with respect to \mathbf{a} and a_0 and setting the results into zero [29, 30, 28] (after some algebraic manipulations) we obtain:

$$a_j^{(new)} = \frac{(N_{ch}N_s) - a_j \sum_{i=1}^{(N_{ch}N_s)} \Sigma_{i,(j,j)}}{\sum_{i=1}^{(N_{ch}N_s)} \mu_{i,j}}, j = 1, 2, \dots, 2N_sN_h \quad (15)$$

$$a_0^{(new)} = \frac{\sum_{i=1} N_{ch}N_s \left(N_t - 2N_sN_h + \sum_{j=1}^{2N_sN_h} a_j \Sigma_{i,(j,j)} \right)}{\sum_{i=1}^{N_{ch}N_s} \|\mathbf{y}_i - \boldsymbol{\Phi}_i \boldsymbol{\mu}_i\|_2^2} \quad (16)$$

where $\mu_{i,j}$ the j -th element of $\boldsymbol{\mu}_i$ and $\Sigma_{i,(j,j)}$ the j -th diagonal element of covariance matrix $\boldsymbol{\Sigma}_i$. The above analysis suggests an iterative algorithm that iterates between Eqs. (12), (13), (15) and (16), until a convergence criterion is satisfied. Also, the same algorithm can be derived by adopting the EM framework and treating parameters \boldsymbol{w}_i as hidden variables[29]. Finally, based on the above bayesian formulation, we can derive a fast version of the above algorithm. The fast version provides an elegant treatment of feature vectors by constructing adaptively the matrix $\boldsymbol{\Phi}$ through three basic operators: addition, deletion and re-estimation. More information on this subject can be found in [29, 28].

Now, SSVEP components in each task can be represented as:

$$\hat{\boldsymbol{y}}_i = \boldsymbol{\Phi}\boldsymbol{\mu}_i, i = 1, \dots, N_{ch}N_s$$

rearranging filtered EEG signals, $\hat{\boldsymbol{y}}_i$, each filtered EEG trial is represented as: $\mathbf{X}_m^{\mathbf{f}(s)} = \mathbf{X}_m^{(s)}a_0\boldsymbol{\Phi}\boldsymbol{\Sigma}_i\boldsymbol{\Phi}^\top$. Due to filtered trials we find the spatial filters \mathbf{w}_s by solving the following generalized eigenvalue problem:

$$\max_{\mathbf{w}_s} \frac{\mathbf{w}_s^\top A_f A_f^\top \mathbf{w}_s}{\mathbf{w}_s^\top B_f B_f^\top \mathbf{w}_s} \quad (17)$$

where $A_f = \frac{1}{M} \sum_{m=1}^M \mathbf{X}_m^{\mathbf{f}(s)}$, and B_f is a concatenated matrix contains all trials of s -th stimulus, $B_f = [\mathbf{X}_1^{\mathbf{f}(s)}, \mathbf{X}_2^{\mathbf{f}(s)}, \dots, \mathbf{X}_M^{\mathbf{f}(s)}]$. The above generalized eigenvalue problem can be connected by that of Eq. 5. After some algebraic manipulations Eq. 17 can be written as:

$$\max_{\mathbf{w}_s} \frac{\mathbf{w}_s^\top A C A^\top \mathbf{w}_s}{\mathbf{w}_s^\top B D B^\top \mathbf{w}_s} \quad (18)$$

where $C = (a_0\boldsymbol{\Phi}\boldsymbol{\Sigma}_i\boldsymbol{\Phi}^\top)(a_0\boldsymbol{\Phi}\boldsymbol{\Sigma}_i\boldsymbol{\Phi}^\top)^\top$ and $D = \begin{bmatrix} C & \dots & 0 \\ \vdots & \ddots & \vdots \\ 0 & \dots & C \end{bmatrix}$. We can observe an interesting connection between the proposed method and the TRCA.

When the $C = \mathbf{I}$, where \mathbf{I} is the unitary matrix, the proposed approach degraded to the TRCA method. We see that the TRCA method is a limiting case of the proposed method. In addition, we can observe that matrices C and D acts on the time dimension of the EEG trials, hence time samples are differently treated according to the time dimension rather than equally

weighted. Also, we can observe that filters, represented by matrix C , are adapted to the statistical properties of EEG trials. Finally, after finding the spatial filters, to find the target of the test trial, \mathbf{X}_{test}^f we apply the following discriminant function:

$$c = \arg \max_s \{corr(\mathbf{w}_s^\top \mathbf{X}_{test}^f, \mathbf{w}_s^\top A_f)\} \quad (19)$$

2.5. Ensemble case

According to the previous discriminant rule, described by Eq. 19, we can observe that to calculate the similarity of the test trial to the stimulus s first we apply spatial filter \mathbf{w}_s . However, since we have enough calibration trials we can obtain N_s spatial filters for each stimulus [18, 23]. Hence, we can extend our method using an ensemble approach, similar to [18, 23], where all spatial filters for stimulus s are concatenated to create an ensemble spatial filter $\mathbf{W}_s \in \mathbb{R}^{N_{ch} \times N_s}$. Now, in order to find the target of the test trial, \mathbf{X}_{test}^f we apply the following discriminant function:

$$c = \arg \max_s \{corr(\mathbf{W}_s^\top \mathbf{X}_{test}^f, \mathbf{W}_s^\top A_f)\}, \quad (20)$$

where, now, the function $corr(\cdot)$ depicts correlation between matrices.

3. Results

In our study two, publicly available, SSVEP datasets are used to evaluate our method. We call these datasets, the *Speller* dataset and the *EPOC dataset*, and we provide a description of them in the following paragraphs.

Speller dataset [31]: The *Speller* dataset [31] contains 40-target visual stimuli were presented on a 23.6-in LCD monitor. Thirty five healthy subjects (with normal or corrected-to-normal vision) were recruited for the SSVEP experiment. Furthermore, eight of them had experience with using a SSVEP-based BCI speller. EEG signals were recorded with 64 channels according to an extended 10–20 system. In our experiments we have used electrodes from the occipital and parietal-occipital areas (P_z , PO_5 , PO_3 , PO_z , PO_4 , PO_6 , O_1 , O_z , and O_2). During the experiment, each subject completes 6 blocks, where in each block the subject was looking at one of the visual stimuli, indicated by the stimulus program, in a random order for 5s and he/she complete 40 trials corresponding to all 40 targets. Using event triggers, EEG trials were extracted and down-sampled to 250Hz. Furthermore, there trials

have been band-pass filtered to 7-90Hz with an infinite impulse response (IIR) filter using the *filtfilt* function from MATLAB. Additionally, a delay of 140ms in the visual system was considered in our experiments[31].

EPOC dataset [7]: EEG trials, from 11 subjects executing a SSVEP-based experimental protocol, were acquired. The frequencies of visual stimulation were: 6.66Hz, 7.50Hz, 8.57Hz, 10.00Hz and 12.00Hz. EEG trials were recorded using the Emotiv Epoc device, with 14 wireless channels and a sampling rate of 128 Hz. Each subject was asked to gaze at one of the visual stimuli, indicated by the stimulus program, in a random order, and complete 20 trials for each of the five targets. The EEG data have been band-pass filtered from 5Hz to 45Hz. More information about this dataset can be found in [7] and <https://physionet.org/content/mssvepdb/1.0.0/>. The visual latency is an important factor in a SSVEP BCI system. An accurate estimation of the visual latency ensures that the extracted data epochs only contain SSVEP responses to the stimulation. In the *Speller* dataset the visual latency is defined using the classification accuracy[31], while, in the *EPOC dataset* an alignment procedure is used to extract data epochs containing the SSVEP responses.

3.1. Performance metrics

To calculate the performance metrics we adopt a leave-one-out cross-validation scheme where we use $B - 1$ blocks for training and 1 block for testing, similar to [17, 8, 31, 9]. The performance of the examined algorithms was calculated by using the following metrics:

Classification Accuracy: Classification Accuracy is the ratio between the number of correctly classified trials to the total number of trials.

Information Transfer Rate (ITR): When a BCI system is designed, we are interested, besides the accuracy, to the number of classes offered, as well as, to the time required for the classification process. These two factors are particularly important in the design of BCI systems since they determine the amount of information that can be transmitted. Hence, we use an additional metric called Information Transfer Rate (ITR). ITR is used to quantify the rate of information transmitted by the BCI system and is measured by the following equation:

$$ITR = \left(\log_2 K + P \cdot \log_2 P + (1 - P) \log_2 \left[\frac{1 - P}{K - 1} \right] \right) \cdot \left(\frac{60}{T} \right) \quad (21)$$

with K being the number of classes, P the classification accuracy, and T the time in seconds required for the classification process to complete.

We compare the proposed spatial filtering method with two spatial filtering approaches: the CCA[13] and the TRCA[18], and with two ML methods: the MLR approach [8] and the Graph-based Sparse Representations Classification (MLR-SRC) [32]. We have calculate the above metrics with respect the time window of the test EEG trial, the number of EEG channels and the number of training trials.

3.2. Performance Comparison versus the Time Window Length

In the first series of experiments we follow a typical analysis of SSVEP datasets by examine the performance of methods with respect to the time window. More specifically, the performance of methods are evaluated for variable time from 0.5sec to 4sec with step of 0.5sec. In addition for the Speller dataset we use the 9 channels from occipital and parietal - occipital areas (Pz, PO5, PO3, POz, PO4, PO6, O1, Oz, O2), while, for the EPOC dataset we use all available 14 channels, covering the entire brain. In Fig. 1 we provide the obtained results for all comparative methods for the two datasets using the basic channel configuration. We can observed the adTRCA and TRCA methods provides better results from all other methods in both datasets. Also, we can observed that between the adTRCA and TRCA, the adTRCA method has marginally better detection accuracy in the *Speller* dataset, and significant better detection accuracy in the *EPOC* dataset. Similar conclusions can be drawn with respect to the ITR (see Tables 1 and 2). We can observed that for most TWs, the adTRCA methods provides the best ITR among all methods. However, we must point out, that for the *Speller* dataset the best ITR is achieved at TW=0.5s from the adTRCA method, while, for the *EPOC* dataset, the best ITR value is achieved at TWs=0.5s from the TRCA method.

3.3. Performance Comparison using the minimal number of EEG channels

In the second series of experiments we have used the minimal number of EEG channels to evaluate the performance of methods. These EEG channels covering the occipital area depending of the EEG device that had been used in each dataset. More specifically, for the Speller dataset O1, O2 and Oz EEG channels are used, while, for the EPOC dataset, we use O1 and O2 channels. This study could correspond to cases where we are not able to use

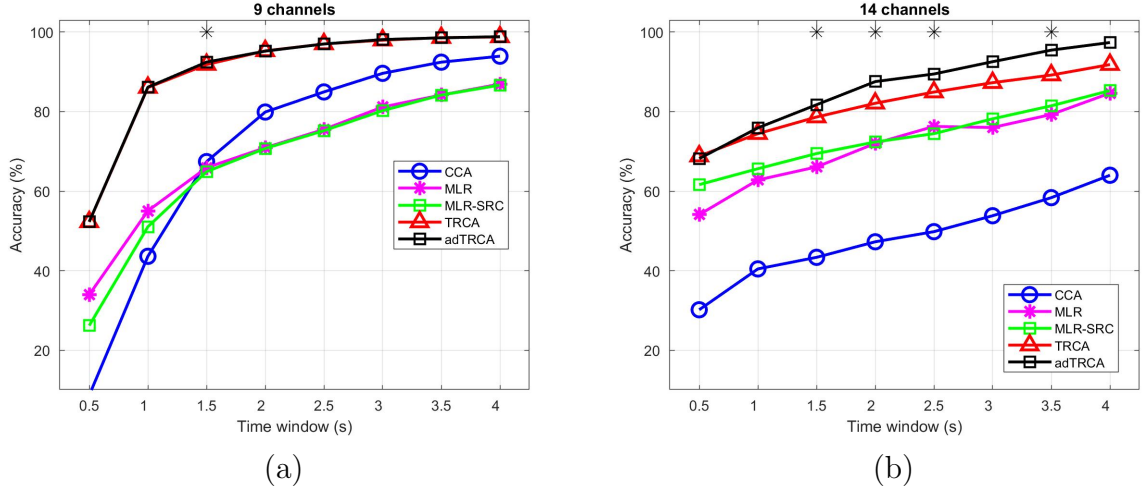


Figure 1: Average Classification over all subjects (a) for the Speller dataset and (b) the EPOC dataset 14 using the basic configuration with respect to the EEG channels. In both cases, the time window ranges from 0.5s to 4s (0.5s interval). * indicates statistically significant difference between the TRCA and adTRCA methods, using paired sample t-test for Speller dataset and Wilcoxon signed rank test for the EPOC dataset ($p < 0.05$).

high density EEG devices such as in BCI applications outside a controlled environment.

In Fig. 2 we provide the obtained results for all comparative methods for the two datasets using the minimal channels' configuration. We can observed the adTRCA and TRCA methods provides better results from all other methods in both datasets. Also, we can observed that between the adTRCA and TRCA, the adTRCA method has better significant better detection accuracy in both datasets. In Tables 3 and 4, we provide the results with respect to the ITR measure for all methods. We can observed that for all TWs, besides ones, the adTRCA methods provides the best ITR among all methods. However, while for the *Speller* dataset the best ITR is achieved at TW=0.5s from the adTRCA method, for the *EPOC* dataset, the best ITR value is achieved at the same TW from the TRCA method.

3.4. Performance Comparison versus the Number of training trials

In the last series of experiments, we investigate how the performance of TRCA and adTRCA are affected by the number of training trials when the time window is 1sec. The obtain results are provided in Tables 5 and 6. The

Table 1: ITR on Speller dataset - 9 channels

TW	CCA	MLR	MLR-SRC	TRCA	adTRCA
0.5	27.3581	141.5439	98.0103	270.9573	271.3097
1	101.8150	137.3785	123.1899	260.0963	260.3216
1.5	122.8637	118.8840	116.4590	189.4191	190.8013
2	116.7986	98.5886	98.1738	149.0613	148.8653
2.5	101.4344	85.9023	85.3361	122.2336	122.1442
3	90.6986	79.0954	77.8773	103.1242	103.3462
3.5	81.1131	71.3472	71.3823	89.2204	89.0756
4	72.5963	65.1814	65.0779	78.2199	78.3041

Table 2: ITR on EPOC dataset - 14 channels

TW	CCA	MLR	MLR-SRC	TRCA	adTRCA
0.5	13.7550	61.4288	81.6831	113.1879	109.7278
1	16.4944	45.1581	49.0298	67.8476	70.7059
1.5	13.3129	35.7231	37.9279	52.7534	55.7158
2	13.6286	31.7665	31.8755	44.0878	48.9809
2.5	12.4521	29.7089	28.1211	38.7167	42.2460
3	12.0830	25.1981	26.2000	35.0314	38.0493
3.5	12.1995	23.8428	24.4427	31.7552	34.8263
4	12.6687	23.6196	23.6422	29.8733	32.1765

proposed method clearly has better accuracy from TRCA. Additionally, the proposed scheme achieves the best performance among them and the margin provided by it is more distinct when a smaller number of training blocks are utilized. Especially, in the case Speller dataset, when only three training blocks are utilized, the proposed scheme achieves a classification accuracy of 63%, while the TRCA method achieve an accuracy of 61%. Furthermore, in the case of EPOC dataset, when three training blocks are used the proposed scheme achieves a classification accuracy of 33%, while the TRCA method achieve an accuracy of 22% (slightly above the random guess).

3.5. Ensemble case - Experiments

In the previous subsection we have presented experiments and we performed comparisons using the basic version of our method. In the current

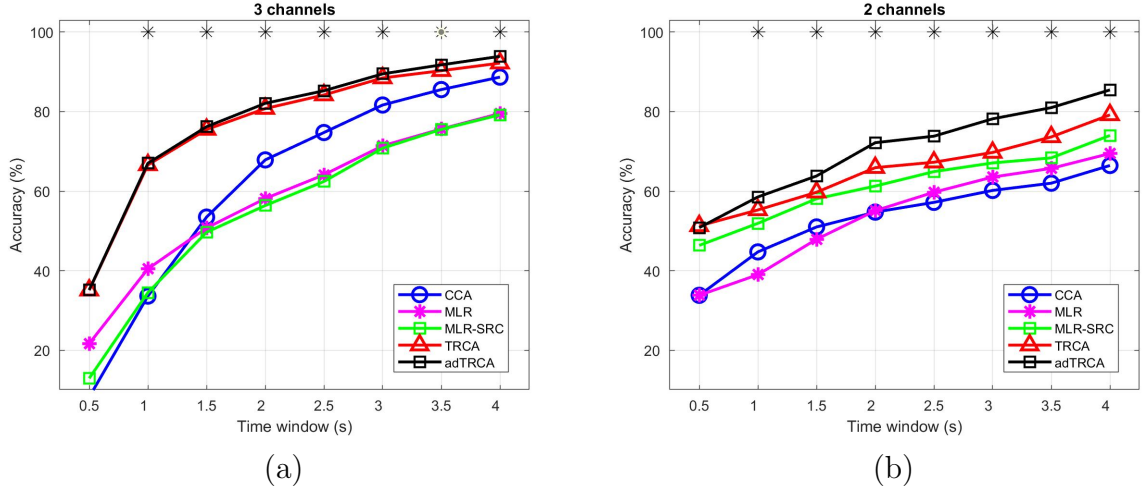
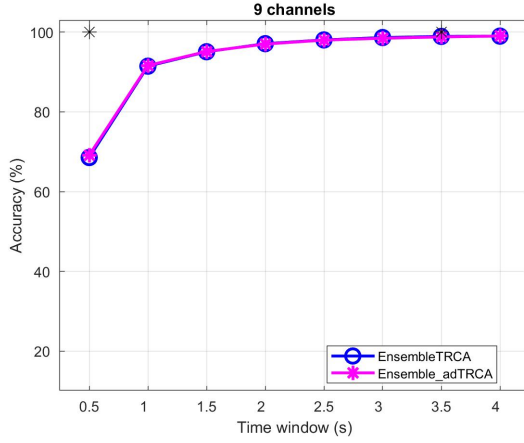


Figure 2: Average Classification over all subjects (a) for the Speller dataset (b) for the EPOC dataset using the EEG channels covering the occipital areas. In both cases, the time window ranges from 0.5s to 4s (0.5s interval). * indicates statistically significant difference between the TRCA and adTRCA methods, using paired sample t-test for Speller dataset and Wilcoxon signed rank test for the EPOC dataset ($p < 0.05$).

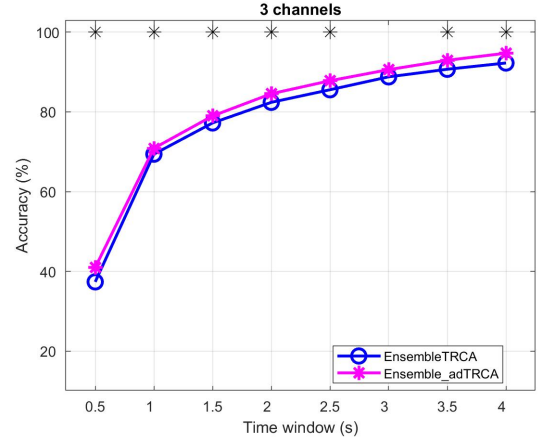
subsection, we provide the obtained results of the ensemble version of our method (see 2.5), and also, we perform a comparison with ensemble TRCA [18]. More specifically, in Fig. 3 we provide the obtained results for the ensemble TRCA (EnsembleTRCA) and ensemble Adaptive TRCA (Ensemble_adTRCA) methods. The comparison between the two methods is performed with respect to the number of channels and the datasets. For the *Speller* dataset we can observe that in the case of 9 channels the two methods present similar performance. However, in the case of 3 channels the Ensemble_adTRCA method provides significantly better performance than the EnsembleTRCA method. Additionally, when we use the *EPOC* dataset, the Ensemble_adTRCA method provides significantly better performance, either using all 14 channels of the EPOC device or the two channels covering the occipital lobe.

4. Discussion and Conclusions

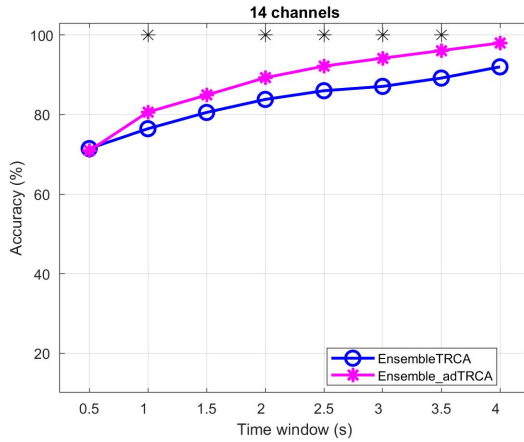
Enhancing the performance of SSVEP recognition is a significant issue for BCI applications. In this study, we develop a multitask learning scheme



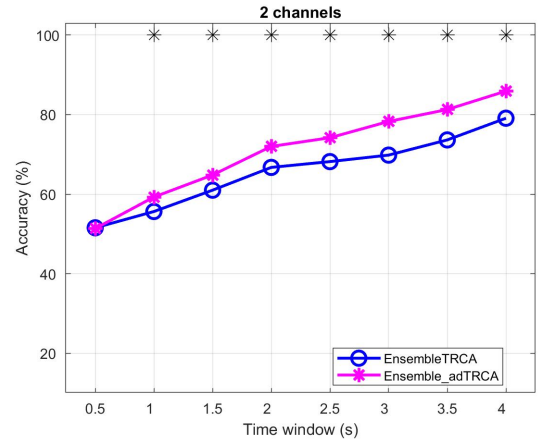
(a)



(b)



(c)



(d)

Figure 3: Average Classification over all subjects by using for the Speller dataset with (a) 9 channels and (b) 3 channels and for the EPOC dataset with (c) 14 channels and (d) 2 channels, respectively. In both cases, the time window ranges from 0.5s to 4s (0.5s interval). * indicates statistically significant difference between the two methods using paired sample t-test for Speller dataset and Wilcoxon signed rank test for the EPOC dataset ($p < 0.05$).

Table 3: ITR on Speller dataset - 3 channels

TW	CCA	MLR	MLR-SRC	TRCA	adTRCA
0.5	26.6513	82.8903	39.9318	162.8981	163.3228
1	71.6644	93.4390	74.2354	189.5521	190.6936
1.5	89.8807	85.1997	82.2758	148.7973	150.0271
2	93.5801	76.2840	73.1798	121.8152	123.6819
2.5	85.4184	69.7438	67.2738	102.4240	103.7595
3	80.0041	67.1743	66.4061	90.6681	91.6374
3.5	73.1382	62.4800	62.2848	79.6201	81.0671
4	67.1804	58.2207	57.9068	71.3779	72.9298

Table 4: ITR on EPOC dataset - 2 channels

TW	CCA	MLR	MLR-SRC	TRCA	adTRCA
0.5	20.4758	17.7383	41.2960	55.2841	54.7309
1	20.8587	13.2992	29.1648	34.8970	38.5391
1.5	20.2541	16.2247	26.1393	29.4451	31.4028
2	18.8570	16.9955	21.9714	27.6870	31.5392
2.5	16.7189	17.8696	20.5254	23.4503	27.1407
3	15.7776	16.6921	18.1873	20.4231	25.5093
3.5	14.5984	15.0986	16.8087	19.7346	23.7536
4	14.6751	15.3353	17.0919	19.9582	23.4404

to strengthen the TRCA method. The idea behind the proposed learning scheme is to develop a adaptive time - domain filter which can be used to a more general eigenvalue problem than the corresponding problem of TRCA method. The proposed method is able to deal with more general noises and with reduced number of trials as the experiments have shown. However, this increase in performance from our method has an increase also in the computation time of the overall procedure since an iterative method is used to find the adaptive time domain filters.

A significant part of our study is the use of two SSVEP datasets to evaluate our method. Most of SSVEP studies use the Speller dataset to evaluate the proposed methods. However, this dataset was created into a controlled environment with high cost EEG equipment which make difficult to replicate

Table 5: Classification accuracy (%) on Speller dataset with respect to the number of training trials - 9 channels

Num	TRCA	adTRCA
3	61.5714	63.0238
4	82.9429	83.3000
5	82.9429	83.3000
6	86.0476	86.1429

Table 6: Classification accuracy (%) on EPOC dataset with respect to the number of training trials - 2 channels

Num	TRCA	adTRCA
3	22.4242	33.3333
7	36.8831	39.4805
10	37.6364	39.8182
15	42.7879	42.7879
20	54.5455	55.2727

the study for real BCI applications with low cost equipment and in very noisy environment. Hence the aforementioned methods that are evaluated on the Speller dataset tend to underestimate the noise part of SSVEP EEG trials. An effect which can be observe by comparing the performance of adTRCA and TRCA on both datasets. We can see that adTRCA method provides much better performance than the TRCA in the case of EPOC dataset. In the Speller dataset the adTRCA method has around 1% better accuracy than the TRCA, while, in the EPOC dataset this difference is increase to 5%. Additionally, the ensemble version of our method presents better performance than the ensemble version of TRCA in both datasets, especially when we have a limited number of channels.

The spatial filters and the SSVEP templates play important roles in the target recognition methods. When the spatial filters and the SSVEP templates can not be accurately computed, e.g. in the case of small calibration data or noisy EEG recordings, the resulting recognition performance will be dramatically decreased. Hence, to this challenge the key is how to estimate reliable spatial filters. In this study, we present a novel spatial filtering approach to recognize SSVEP signals. Our method use the multi-task idea to

construct adaptive time - domain filters resulting into a generalized eigenvalue problem from where the final spatial filters are obtained. Extensive experiments, using two SSVEP datasets, have been shown the usefulness of our method. The proposed method significantly outperformed the TRCA, the CCA, the MLR and the SRC methods in terms of classification accuracy and ITR. Finally, future extensions of our approach could include transfer learning approaches utilizing the data from all subjects to construct the recognition model.

Acknowledgments

This work was part of project NeuroMkt that had been co-financed by the European Regional Development Fund of the European Union and Greek National Funds through the Operational Program Competitiveness, Entrepreneurship and Innovation, under the call RESEARCH CREATE INNOVATE (Project code T2EDK-03661)

Data Availability Statement

The datasets that have been used in this study are available in the Internet. The *Speller* dataset can be found in <http://bci.med.tsinghua.edu.cn/download.html>. The *EPOC* dataset can be found in <https://physionet.org/content/mssvepdb/1.0.0/>.

References

- [1] J. R. Wolpaw, N. Birbaumer, D. J. McFarland, G. Pfurtscheller, T. M. Vaughan, Brain computer interfaces for communication and control, *Clinical Neurophysiology* 113 (6) (2002) 767 – 791.
- [2] L. F. Nicolas-Alonso, J. Gomez-Gil, Brain computer interfaces, a review, *Sensors* 12 (2) (2012) 1211–1279. doi:10.3390/s120201211.
URL <https://www.mdpi.com/1424-8220/12/2/1211>
- [3] F. P. Kalaganis, K. Georgiadis, V. P. Oikonomou, N. A. Laskaris, S. Nikolopoulos, I. Kompatsiaris, Unlocking the subconscious consumer bias: A survey on the past, present, and future of hybrid eeg schemes in neuromarketing, *Frontiers in Neuroergonomics* 2 (2021). doi:10.3389/fnrgo.2021.672982.
URL <https://www.frontiersin.org/article/10.3389/fnrgo.2021.672982>

- [4] G. Bin, X. Gao, Y. Wang, B. Hong, S. Gao, VEP-based brain-computer interfaces: time, frequency, and code modulations , *IEEE Computational Intelligence Magazine* 4 (4) (2009) 22–26.
- [5] R. Zerafa, T. Camilleri, O. Falzon, K. P. Camilleri, To train or not to train? a survey on training of feature extraction methods for SSVEP-based BCIs, *Journal of Neural Engineering* 15 (5) (2018) 051001. doi: 10.1088/1741-2552/aaca6e.
URL <https://doi.org/10.1088/1741-2552/aaca6e>
- [6] S. Gao, Y. Wang, X. Gao, B. Hong, Visual and Auditory Brain Computer Interfaces, *IEEE Transactions on Biomedical Engineering* 61 (5) (2014) 1436–1447.
- [7] V. P. Oikonomou, G. Liaros, K. Georgiadis, E. Chatzilari, K. Adam, S. Nikolopoulos, I. Kompatsiaris, Comparative evaluation of state-of-the-art algorithms for SSVEP-based BCIs, arXiv:1602.00904 (February 2016).
- [8] H. Wang, Y. Zhang, N. R. Waytowich, D. J. Krusienski, G. Zhou, J. Jin, X. Wang, A. Cichocki, Discriminative feature extraction via multivariate linear regression for ssvep-based bci, *IEEE Transactions on Neural Systems and Rehabilitation Engineering* 24 (5) (2016) 532–541. doi:10.1109/TNSRE.2016.2519350.
- [9] V. P. Oikonomou, S. Nikolopoulos, I. Kompatsiaris, A bayesian multiple kernel learning algorithm for ssvep bci detection, *IEEE Journal of Biomedical and Health Informatics* 23 (5) (2019) 1990–2001.
- [10] H. Cecotti, A time-frequency convolutional neural network for the offline classification of steady-state visual evoked potential responses, *Pattern Recognition Letters* 32 (8) (2011) 1145 – 1153.
- [11] N.-S. Kwak, K. Muller, S.-W. S.-W.Lee, A convolutional neural network for steady state visual evoked potential classification under ambulatory environment, *PLOS ONE* 12 (2) (2017) 1–20. doi:10.1371/journal.pone.0172578.
- [12] H. Wang, T. Li, Z. Huang, Remote control of an electrical car with SSVEP-Based BCI, in: 2010 IEEE International Conference on In-

- formation Theory and Information Security, 2010, pp. 837–840. doi: 10.1109/ICITIS.2010.5689710.
- [13] Z. Lin, C. Zhang, W. Wu, X. Gao, Frequency Recognition Based on Canonical Correlation Analysis for SSVEP-Based BCIs, *IEEE Transactions on Biomedical Engineering* 53 (12) (2006) 2610–2614.
- [14] O. Friman, I. Volosyak, A. Graser, Multiple Channel Detection of Steady-State Visual Evoked Potentials for Brain-Computer Interfaces, *IEEE Transactions on Biomedical Engineering* 54 (4) (2007) 742–750.
- [15] Y. Zhang, G. Zhou, J. Jin, M. Wang, X. Wang, A. Cichocki, L1-Regularized Multiway Canonical Correlation Analysis for SSVEP-Based BCI, *IEEE Transactions on Neural Systems and Rehabilitation Engineering* 21 (6) (2013) 887–896.
- [16] G. Bin, X. Gao, Y. Wang, Y. Li, B. Hong, S. Gao, A high-speed BCI based on code modulation VEP, *Journal of Neural Engineering* 8 (2) (2011) 025015.
URL <http://stacks.iop.org/1741-2552/8/i=2/a=025015>
- [17] M. Nakanishi, Y. Wang, Y. Wang, T. Jung, A Comparison Study of Canonical Correlation Analysis Based Methods for Detecting Steady-State Visual Evoked Potentials, *PLoS ONE* (2015) e0140703doi:10.1371/journal.pone.0140703.
- [18] M. Nakanishi, Y. Wang, X. Chen, Y.-T. Wang, X. Gao, T.-P. Jung, Enhancing detection of ssveps for a high-speed brain speller using task-related component analysis, *IEEE Transactions on Biomedical Engineering* 65 (1) (2018) 104–112. doi:10.1109/TBME.2017.2694818.
- [19] C. Tong, H. Wang, C. Yang, X. Ni, Group ensemble learning enhances the accuracy and convenience of ssvep-based bcis via exploiting inter-subject information, *Biomedical Signal Processing and Control* 68 (2021) 102797.
- [20] X. Yuan, Q. Sun, L. Zhang, H. Wang, Enhancing detection of ssvep-based bcis via a novel cca-based method, *Biomedical Signal Processing and Control* 74 (2022) 103482.

- [21] V. P. Oikonomou, S. Nikolopoulos, I. Kompatsiaris, Machine-learning techniques for eeg data, *Signal Processing to Drive Human-Computer Interaction: EEG and eye-controlled interfaces* (2020) 145.
- [22] C. M. Wong, B. Wang, Z. Wang, K. Lao, A. Rosa, F. Wan, Spatial filtering in ssvep-based bcis: Unified framework and new improvements, *IEEE Transactions on Biomedical Engineering* 67 (11) (2020) 3057–3072. doi:10.1109/TBME.2020.2975552.
- [23] Y. Zhang, D. Guo, F. Li, E. Yin, Y. Zhang, P. Li, Q. Zhao, T. Tanaka, D. Yao, P. Xu, Correlated component analysis for enhancing the performance of ssvep-based brain-computer interface, *IEEE Transactions on Neural Systems and Rehabilitation Engineering* 26 (5) (2018) 948–956.
- [24] B. Liu, X. Chen, N. Shi, Y. Wang, S. Gao, X. Gao, Improving the performance of individually calibrated ssvep-bci by task- discriminant component analysis, *IEEE Transactions on Neural Systems and Rehabilitation Engineering* 29 (2021) 1998–2007. doi:10.1109/TNSRE.2021.3114340.
- [25] C. M. Wong, F. Wan, B. Wang, Z. Wang, W. Nan, K. F. Lao, P. U. Mak, M. I. Vai, A. Rosa, Learning across multi-stimulus enhances target recognition methods in SSVEP-based BCIs, *Journal of Neural Engineering* 17 (1) (2020) 016026. doi:10.1088/1741-2552/ab2373. URL <https://doi.org/10.1088/1741-2552/ab2373>
- [26] J. Jin, Z. Wang, R. Xu, C. Liu, X. Wang, A. Cichocki, Robust similarity measurement based on a novel time filter for ssveps detection, *IEEE Transactions on Neural Networks and Learning Systems* (2021) 1–10doi:10.1109/TNNLS.2021.3118468.
- [27] L. Sun, S. Ji, J. Ye, *Multi-Label Dimensionality Reduction*, CRC Press, Taylor and Francis Group, 2014.
- [28] S. Ji, D. Dunson, L. Carin, Multitask compressive sensing, *IEEE Transactions on Signal Processing* 57 (1) (2009) 92–106. doi:10.1109/TSP.2008.2005866.
- [29] M. E. Tipping, Sparse Bayesian Learning and the Relevance Vector Machine, *Journal of Mach. Learn. Research* 1 (2001) 211–244.

- [30] D. J. MacKay, Bayesian interpolation, *Neural Computation* 4 (1992) 415–447.
- [31] Y. Wang, X. Chen, X. Gao, S. Gao, A benchmark dataset for SSVEP-based brain - computer interfaces, *IEEE Transactions on Neural Systems and Rehabilitation Engineering* 25 (10) (2017) 1746–1752. doi:10.1109/TNSRE.2016.2627556.
- [32] V. P. Oikonomou, S. Nikolopoulos, I. Kompatsiaris, Sparse graph-based representations of ssvp responses under the variational bayesian framework, in: *2021 IEEE 21st International Conference on Bioinformatics and Bioengineering (BIBE)*, 2021, pp. 1–6. doi:10.1109/BIBE52308.2021.9635427.